Copyright © 2012 Tech Science Press CMES, vol.89, no.2, pp.123-141, 2012

On the Use of PEBI Grids in the Numerical Simulations of Two-Phase Flows in Fractured Horizontal Wells

Yongsheng An[1], Xiaodong Wu[1] and Deli Gao[1]

Abstract: The accuracy of numerical simulation of a two-phase (oil and water) flow in a fractured horizontal well depends greatly upon the types of grids used in the computation. Cartesian grids have been widely used in recent years, but they have some disadvantages in describing complex structural wells, such as fractured horizontal wells. For example, Cartesian grids are not efficient in describing the main wellbores and the fractures of fractured horizontal wells, and the results can frequently suffer from grid orientation effects, even though a grid-refinement is often introduced to enhance the adaptability of a Cartesian grid.

The PEBI (Perpendicular Bisector) grid is defined as a region which is closer to its grid point than any other grid points of the space, and it is locally orthogonal, i.e. the block boundaries are normal to the lines joining the nodes on the two sides of the boundary. The PEBI grid is more flexible than a Cartesian grid and it can be constructed according to the orientation of the wellbores and the fractures, which feature is very important to simulate the multi-phase flow near the fractured horizontal wells. Moreover, the characteristic of PEBI grid allows for a fine-scale gridding near the wellbores and the fractures.

A hybrid PEBI grid (a combination of Cartesian grid and a hexagonal grid) is presented in this paper. A Cartesian grid and hexagonal grid are used to simulate the region of the fractured horizontal wells, and the region of the reservoir, respectively. It is found that the more flexible aspects of the hybrid PEBI grid system allow for a better grid construction near the fractured horizontal wells. The fractures as well as the wellbores are better simulated in this grid system. An example of a five-spot well pattern of a fractured horizontal well is presented in this paper.

Keywords: Numerical simulation; fractured horizontal well; PEBI grid; Cartesian grid; five-spot well pattern

[1] Key Lab of Petroleum Engineering in the Ministry of Education, China University of Petroleum, Beijing 102249, China. Corresponding author: Deli GAO and Yongsheng An. E-Mail: gaodeli@cup.edu.cn; an_yongsheng@126.com

1 Introduction

A Cartesian coordinate system is used in most reservoir simulators, and this has the advantages of simplicity, rapidity, and accuracy. The reservoir can be divided into a block centered grid and a point centered grid. However, when the reservoir problems are simulated using Cartesian grids, a fine grid-spacing is often necessary when the pressure gradients are high. Such a local grid refinement is often used in places where a coarse grid is not sufficient such as in the vicinity of the wells, boundaries or faults [Chen et al. (2011) and Liu et al. (2012)]. The use of a local grid refinement can improve the accuracy greatly, but it also requires a more complex finite difference approximation and a more ill-conditioned matrix.

Modeling complex structural wells is very difficult using Cartesian grids, because the track of the wellbore is so arbitrarily shaped, that the Cartesian blocks cannot capture it very well, even when a local grid refinement is used, and the flow cannot be simulated precisely. A more flexible grid system should be used to deal with such complex geometries. Such alternate grid systems include the hybrid grid and PEBI (Perpendicular Bisector) grid.

With the purpose of improving the treatment of wells in numerical simulators, Pedrosa et al. (1986) proposed a method that involves using a rectangular Cartesian grid in the reservoir, and using a curvilinear grid in the vicinity of the vertical wells A special treatment is used to bridge these two grid systems. This grid system is also called the hybrid grid system.

The PEBI grid technique was introduced into the field of reservoir numerical simulation, as early as 1991 by Heinemann et al. (1991). They formulated the flow equations for a grid block with any number of connections, and proposed an algorithm which generates an irregular hexagonal grid. They found that the grid orientation effects are more insignificant when a PEBI grid is used, than when a Cartesian grid is used.

Because a PEBI grid is more flexible than a Cartesian grid, it is used very frequently in literature. Palagi et al. (1993) applied the PEBI grid to model flow in a heterogeneous reservoir, and proposed a new grid generation procedure and a new technique to specify physical properties. Verma and Aziz (1997) presented a method to construct two dimensional or three dimensional flexible grids for reservoir simulations, and also presented numerical schemes to solve the fluid flow equations on these grids. Pattay and Ganzer (2001) implemented a dual porosity and a dual permeability system into the PEBI grid simulation. They presented a reservoir simulation model for fractured and partially fractured reservoirs, based on the PEBI grid.

Recently, the PEBI grid technique was applied more and more frequently. Melichar

et al. (2003) applied the PEBI grid for a heavily faulted reservoir in the Gulf of Mexico. They found that the PEBI grid was more practical than Cartesian or curvilinear grids, for that particular case, because the PEBI grid allowed a more accurate and flexible modeling complex-shaped structural reservoir.

Vestergaard et al. (2008) applied the PEBI grid techniques for full-field simulations of a giant carbonate reservoir which was developed with long horizontal wells. They presented a gridding study for a complex, low permeability carbonate reservoir, which was developed with seventy-five ultra-long horizontal wells. A process of selecting a suitable grid for matching the history was proposed.

Gonzalez et al. (2009) studied the simulation of steamflooding, with horizontal producers, based on the PEBI grid techniques. They concluded that the PEBI grid is suitable to represent adverse displacement phenomena, thereby reducing the grid-orientation effects. Horizontal production wells created a more uniform pressure drawdown distribution around the hexagonal perimeter.

The Perpendicular Bisector (PEBI) gridding technique is a powerful tool for modeling complex-shaped reservoirs and complex-shaped structural wells. In this study, the PEBI grid is applied to simulate a fractured horizontal well which is a special case of complex structural wells. A method of generation of the PEBI grid is carried out, which assures that the main wellbore and the fractures are positioned properly in the grid system according to the structure of the fractured horizontal well. Studies of the distribution of oil saturation in a five spot well pattern, including a fractured horizontal producer and four vertical injectors, are carried out.

The proposed method of generation of the PEBI grid helps us to establish a numerical model for fractured horizontal wells in which the flow near the wellbores and the fractures can be simulated more precisely [Deng et al. (2011)]. Based on this model, the mechanism of percolation in fractured horizontal wells can be studied.

2 Methods of Construction of PEBI Grids

As compared with the Cartesian grid, the greatest advantage of PEBI grid is its flexibility in grid point distributions. Meanwhile, the simulation accuracy is highly dependent on how the grids are generated; hence it is critical to optimize the PEBI grids. In this section we propose a new technique for the PEBI grid generation, for generating the grid point locations based on the wellbore and the fractures, and for targeting the configurations of fractured horizontal wells.

2.1 Generating the PEBI Grid Nodes

1. The Process of Generating PEBI Grid Nodes.

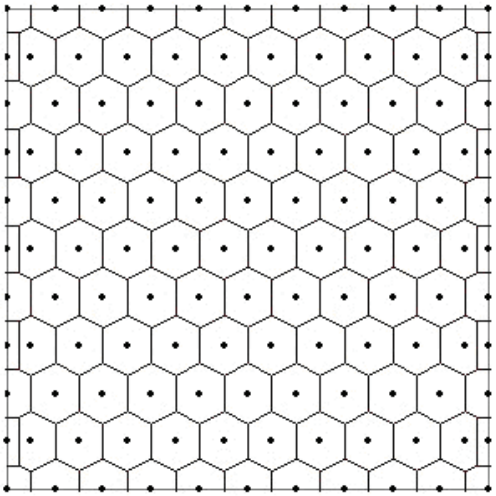

Figure 1: PEBI grid based on a hexagonal grid

(a) Select a region to be simulated, and set evenly distributed PEBI grids in the whole region as background grids, and record the coordinates of the nodes of the grid.

(b) Distribute Cartesian grids evenly near the wellbore of the fractured horizontal well, and record the coordinates of the grid nodes.

(c) Distribute Cartesian grids by the shape and location of the fracture, and record the coordinates of the grid nodes.

(d) Calculate the distance d_{ij} between the background grid nodes and the non-background grid nodes from the above steps, respectively. If d_{ij} is smaller than d_{min}, the corresponding background grid nodes should be removed.

(e) Record the number of boundary nodes and internal nodes, as well as the planar coordinates of all the grid-nodes.

2. The process of treating the intersection of the fracture and the wellbore.

   The generated grid system is complicated, due to the large quantity of points of intersection of the artificial fracture and the wellbore of the fractured horizontal well, which causes the fracture-simulation grids to be distorted easily. Therefore, it is necessary to treat these grid points in a special way. See Fig.2 It is done as follows:

(a) According to the location of the fracture of fractured horizontal well, determine, E(x, y), the point of intersection of the centerline of the fracture and the wellbore in the model.

(b) Derive the equation of line l_1 of the centerline of the fracture, using the angle θ between the fracture and the wellbore, and the coordinates of E.

(c) Calculate the coordinates of Q, the point of intersection of $l_1$and l_2.

(d) Determine the coordinates of P_1 and P_2 based on the coordinates of Q.

(e) Calculate the coordinates of P_3 from the coordinates of P_1 and the equation of l_1, since P_1 and P_3 are symmetric about the line l_1.

(f) Plot the line $l_3$that parallels the fracture and passes through the point P_1 which intersects with the line l_4, that passes through E and parallels the line P_1P_3, at point A. Then calculate the coordinates of A, and those of B which is symmetric to A about E.

(g) Divide the upper half of the fracture into several equal parts by the fracture half-length, and calculate from P_1, P_2, P_3. We could obtain the coordinates of the other nodes of the upper half of the fracture, based on the length and angle of every equal part.

(h) Determine the nodes which are located in mirror symmetry, to P_1 P_2 and P_3, with reference to the point of intersection E, namely the starting points for the lower half-fracture, and the other nodes points could be obtained subsequently.

3. A process of the gridding of the edge of the fracture

The fluid flow occurring at the edge of a fracture is special, and the PEBI grids at this location will become distorted, without a further special treatment while the grid is being generated, resulting in a severe loss of accuracy, since the distorted grids could not simulate the fluid flow efficiently at the edge of the fracture. The technique we applied is described as follows:

Assume that the angle between the centerlines of a certain fracture and the main wellbore is θ, the fracture width is d, and the coordinates of the nodes of the last row at the fracture-edge are P_{1n}, P_{2n} and P_{3n} respectively. See Fig.3. Grid the fracture edge with equilateral triangulations, and hence $\Delta WP_{2n}R$, $\Delta GP_{2n}R$, $\Delta GP_{2n}V$ are all equilateral triangles, in which W, R, G and V are located on the same circle. It is of great importance to determine the coordinates of O_1, O_2 and O_3 for griding the fracture edge successfully with equilateral triangulations.

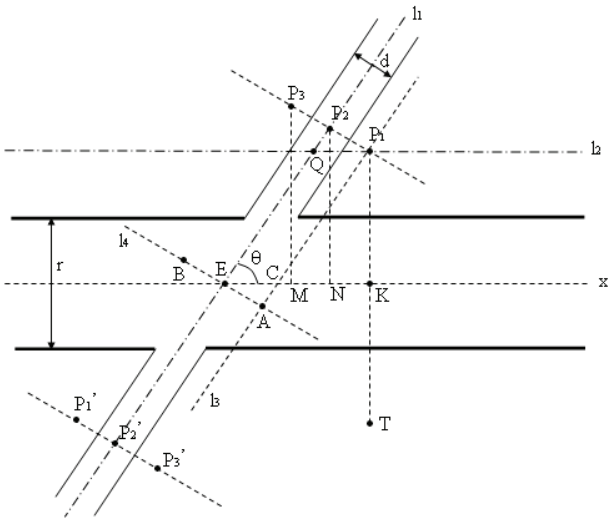

Figure 2: A method of handling the intersection of the fracture and the well bore of fractured horizontal well

(a) Based on the properties of PEBI grid and the analysis above, the coordinates of O_1 can be obtained from the known coordinates of P_{2n}, and knowing that the line $P_{2n}O_1$ is perpendicular to and bisects the line WR.

(b) Calculate the coordinates of O_2 from $\Delta P_{2n}WR$ and $\Delta P_{2n}O_2F$.

(c) From the equation of the line l_5 as formulated by θ and the coordinates of P_{2n}, the coordinates of O_3 can be determined since O_3 is located symmetrically with O_1, about the line l_5.

2.2 Delaunay Triangulation

Delaunay triangulation is a method of quickly generating triangular grids in discretized point series. Embed one point P into the Delaunay triangulated grid with the Bowyer-Watson algorithm, then find out and delete the triangular elements including P in all circumscribed circles, and generate one Delaunay cavity. Finally, connect P with all the points on the wall of Delaunay cavity and a new Delaunay triangulation is formed.

According to the principles above, the process is concluded as follows:

(a) Ensure that all the grid nodes are enclosed in the triangles, by constructing a super-large triangle.

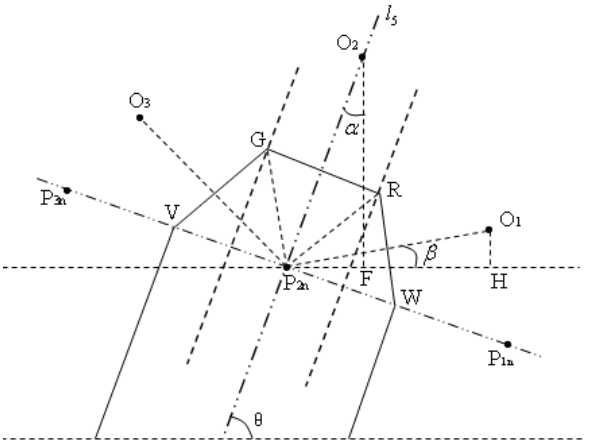

Figure 3: Grid dividing method of the end point of fracture

(b) Choose the super-large triangle as the first member in the triangle set D.

(c) For any arbitrary point in the discretized point set, search the triangle set T in the triangle set D, that could form a circumscribed circle with the point being included.

(d) Construct a triangle set N using the new point and the corner points of the triangle set T, and replace T with N in the triangle set D.

(e) Repeat step 3 and 4 until all convergent points of discretized points are added into the triangle set D.

(f) Remove all the triangles relevant to super-large triangles from the triangle set D.

During this grid generating process, we need to input the coordinates of every grid node. Fig.4 shows the generated Delaunay triangle. Based on the experience of generating Cartesian grid, it is advisable to reduce the orientation effects by reducing the ratio of the grid length to the grid width. Therefore, the optimal triangle is recommended to be an equilateral. Record all the information about every point of triangle after Delaunay triangles are generated.

2.3 Generating the PEBI Grid

For any arbitrary grid node, the process of generating the PEBI grid is summarized as follows:

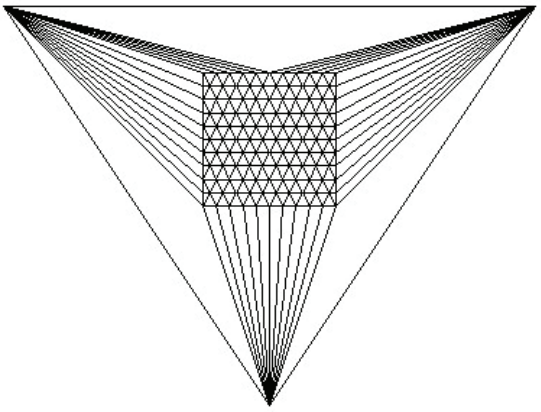

Figure 4: A schematic diagram of Delaunay Triangulation

(a) If the node is internal, construct the PEBI grid by connecting the ex-centers of Delaunay triangles, which are generated with the internal node and the neighboring nodes, counter-clockwise.

(b) If the node is a boundary node, construct the PEBI grid by joining counter-clockwise, the ex-centers of Delaunay triangles and the midpoint between the boundary node and neighboring node, and the Delaunay triangle is obtained by connecting the boundary node, the internal point and the midpoint between the boundary node and adjacent node.

Consider two examples of fracture number 4 and θ for 90° and 45° respectively, where θ is the angle between the fracture and the wellbore apply the technique above to construct PEBI grids. The results are showed in Fig.5.

3 Numerical Model

3.1 Fundamental mathematic equation

In a two-phase flow, given that the oil and water phases are slightly compressible and that there is no loss of mass in the fluid flow process for any unit block, the material balance equations are as follows:

$$-\nabla\left(\frac{v_o}{B_o}\right) - q_o = \frac{\partial}{\partial t}\left(\frac{\phi S_o}{B_o}\right) \tag{1}$$

$$-\nabla\left(\frac{v_w}{B_w}\right) - q_w = \frac{\partial}{\partial t}\left(\frac{\phi S_w}{B_w}\right) \tag{2}$$

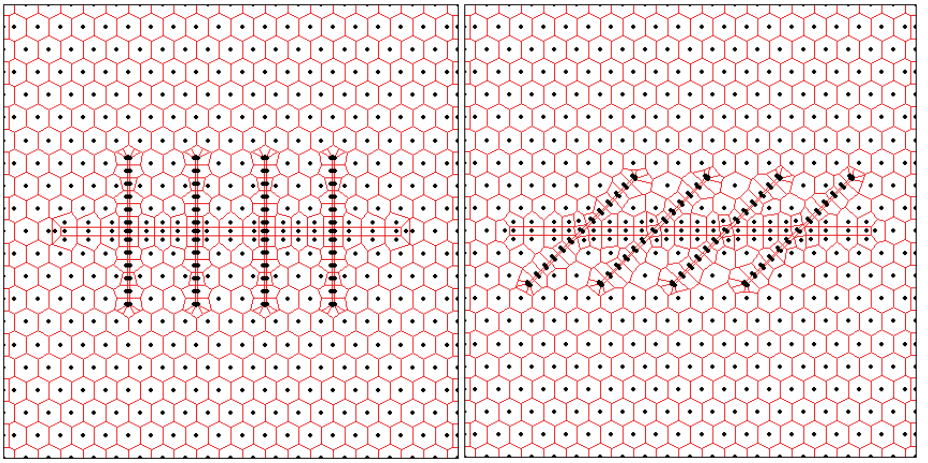

Figure 5: PEBI grid of fractured horizontal wells

Where v_o and v_w are the oil flow rate and the water flow rate respectively (m/s), B_o and B_w are the oil volume factor and water volume factor (single), S_o and S_w are the oil saturation and water saturation (single), q_o and q_w are the oil volume flow rate and water volume flow rate under standard conditions(the direction of flowing out denotes positive) (1/s).

The oil-water two phase flow rates satisfy the Darcy's law accounting for the gravity effect:

$$v_o = -\frac{KK_{ro}}{\mu_o}\nabla\left(p_o - \rho_o g D\right) \tag{3}$$

$$v_w = -\frac{KK_{rw}}{\mu_w}\nabla\left(p_w - \rho_w g D\right) \tag{4}$$

Where K is the absolute permeability ($10^3 \mu m^2$), K_{ro} and K_{rw} are the relative permeabilities of oil and water respectively(dimensionless), μ_o and μ_w are oil viscosity and water viscosity respectively (mPa·s), p_o and p_w are oil phase pressure and water phase pressure (MPa), $\rho_o$and ρ_w are oil density and water density (kg/m^3) respectively, g is the acceleration of gravity (m/s^2), D is the depth (the downward direction denotes positive) (m).

The oil and water flow equations can be obtained by substituting Eq.3 and Eq.4 into Eq.1 and Eq.2 respectively:

$$\nabla\left[\frac{KK_{ro}}{B_o\mu_o}\nabla\left(p_o - \rho_o g D\right)\right] - q_o = \frac{\partial}{\partial t}\left(\frac{\phi}{B_o}S_o\right) \tag{5}$$

$$\nabla\left[\frac{KK_{rw}}{B_w\mu_w}\nabla\left(p_w-\rho_w gD\right)\right]-q_w=\frac{\partial}{\partial t}\left(\frac{\phi}{B_w}S_w\right) \tag{6}$$

Auxiliary equations:

$$S_o+S_w=1 \tag{7}$$

$$p_{cow}=p_o-p_w \tag{8}$$

Initial conditions:

$$p_o\left(x,y,z,t\right)|_{t=t_0}=p_o^0,\quad S_w\left(x,y,z,t\right)|_{t=t_0}=S_w^0 \tag{9}$$

Boundary conditions:

$$\left.\frac{\partial p_o}{\partial n}\right|_\Omega=0,\quad \left.\frac{\partial S_w}{\partial n}\right|_\Omega=0 \tag{10}$$

This paper would apply a fully implicit technique to construct the coefficient matrix. Discretize the oil and water flow equations:

$$\sum\left(\frac{K_{ro}}{\mu_o B_o}\right)^{n+1}T_{ij}\left(\Phi_{oj}^{n+1}-\Phi_{oi}^{n+1}\right)-Q_o^{n+1}=\frac{V_i}{\Delta t}\left[\left(\left(\frac{\phi}{B_o}S_o\right)^{n+1}-\left(\frac{\phi}{B_o}S_o\right)^{n}\right)\right] \tag{11}$$

$$\sum\left(\frac{K_{rw}}{\mu_w B_w}\right)^{n+1}T_{ij}\left(\Phi_{wj}^{n+1}-\Phi_{wi}^{n+1}\right)-Q_w^{n+1}=\frac{V_i}{\Delta t}\left[\left(\left(\frac{\phi}{B_w}S_w\right)^{n+1}-\left(\frac{\phi}{B_w}S_w\right)^{n}\right)\right] \tag{12}$$

$$T_{ij}=K_{ij}\frac{Area_{ij}}{d_{ij}} \tag{13}$$

Where Φ_o and Φ_w represent the potential of water and oil, V_i represents the volume of grid i, $Area_{ij}$ represents the area of surface of grid between node i and node j, d_{ij} represents the distance form node i to node j.

Calculate K_{rp}, μ_p and B_p at the interface between node i and node j with the upper-stream weight method, and average the absolute permeability$K$ by the permeability of adjacent nodes with harmonic mean method, namely,

$$K_{ij}=\frac{2K_iK_j}{K_i+K_j} \tag{14}$$

3.2 The process of treating a fracture

The main reason for a high oil production, based on the fractured horizontal well in a low permeability reservoir, is the high permeability in the fracture, resulting in a more effective flow channel.

Generally, width of a fracture ranges from 3mm to 5mm, and the scale of the grid in the reservoir is much larger than the scale of the grid in the fracture, leading to a higher permeability and volume flow rate in the small fracture-grid. Therefore, if we don't solve this problem, the numerical stability of the simulation will be influenced, and even cause convergence not to be achieved.

This paper employed an equivalent-fracture-flow-conductivity method to handle the problems posed by smaller fracture grids. The formula for the flow conductivity of a fracture is expressed as follows:

$$f_{rcd} = K_f \cdot w_f \tag{15}$$

Where f_{rcd} represents the flow conductivity of fracture (μm^2·cm), K_f represents the fracture permeability (μm^2), w_f represents the fracture width (cm).

The flow conductivity of a fracture is defined as the product of the fracture width and the fracture permeability. To avoid the negative influence on simulation caused by the fact that fracture permeability is much larger than the reservoir permeability, we could magnify the fracture-width appropriately and reduce the fracture permeability, as the flow conductivity is constant in griding, causing the solution to become more stable and achieve convergence more quickly.

3.3 Grid ranking method

For the PEBI grid, the biggest advantage is its flexibility in distributing the grid nodes, but the constraints are that the location is not fixed and the number of neighboring nodes of each node is not equal to each other, resulting in the band-width of the coefficient matrix of equations to be not desirable. Consequently, it is more difficult to store data during the calculation.

Aiming to efficiently find, record and handle the nodes of PEBI grid system of fractured horizontal well, we rank the grids by row and column. Consider the example of a grid system based on one horizontal well located in the center of single-layer bulk reservoir, rank the grids in a row and column manner, and the configuration of the obtained matrix is shown in Fig.6

4 Application of the PEBI Grid for Fractured Horizontal Wells

We consider a certain low permeability oilfield in west China as an example, and simulate the production performance of a fractured horizontal well pattern. We

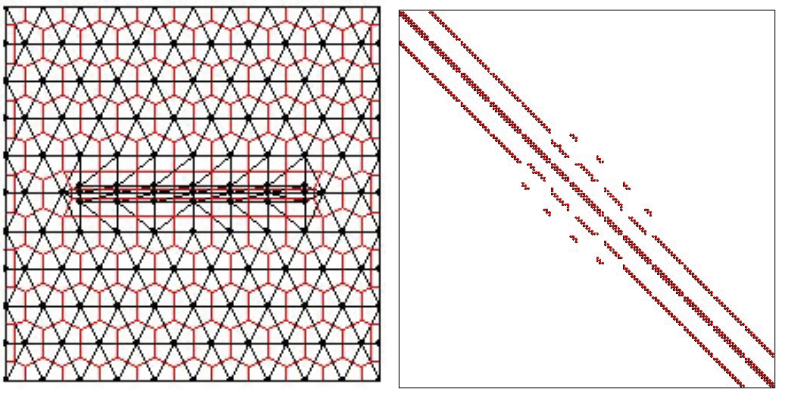

Figure 6: Matrix of PEBI grid

only consider the production in the fracture in the simulation, for comparing the horizontal well fracturing method in the field, that is, the horizontal well segments are closed except where the fracture starts to develop. The basic parameters for the model are presented in Table 1 and Table 2. To enhance the efficiency, a single-layer reservoir is assumed for grid construction and simulation.

Based on the data in Table 1 and Table 2(a=500m, b=250m), the fracture parameters of fractured horizontal wells are optimized under a five-spot well pattern condition See Fig.7.

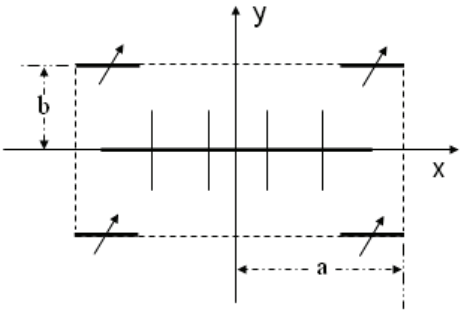

Figure 7: A schematic diagram of fractured horizontal well in a five-spot point well pattern

With the PEBI gird generation technique for fractured horizontal well proposed in this paper, we generated the grid nodes, and constructed the PEBI grid for the well

Table 1: Fundamental parameters

parameter	**value**
Thickness, m	18.0
Depth, m	1898
Reservoir pressure, MPa	15.7
Porosity, %	10.3
Permeability, μm^2	0.002
Water volume factor,dimensionless.	1
Oil volume factor, dimensionless.	1.08
Initial saturation, dimensionless.	0.2
Radius of wellbore, m	0.07
The conductivity of fracture, μm^2·cm	30
Oil density, Kg/ m^3	862.8
Oil viscosity, mPa·s	1.17
Length of injection well, m	200
Number of water injection well	4
Flowing pressure of production well, MPa	5
Flowing pressure of injection well, MPa	25

Table 2: Relationship between relative permeability and water saturation

S_w	K_{ro}	K_{rw}
0.38	1	0
0.45	0.26	0.05
0.5	0.16	0.12
0.55	0.1	0.27
0.6	0.07	0.38
0.65	0.05	0.48
0.7	0.035	0.54
0.75	0.017	0.62
0.8	0	0.68
1	0	1

pattern given previously. We will consider two examples for simulation: facture number 4, θ for 90° and facture number 4, θ for 45°. The oil saturation distribution results for different production phases are shown in Fig.8 and Fig.9.

In Fig.8, the outer fracture edge of the fractured horizontal well is seen to encounter the water first, and the inside two fractures do subsequently. After the two outer

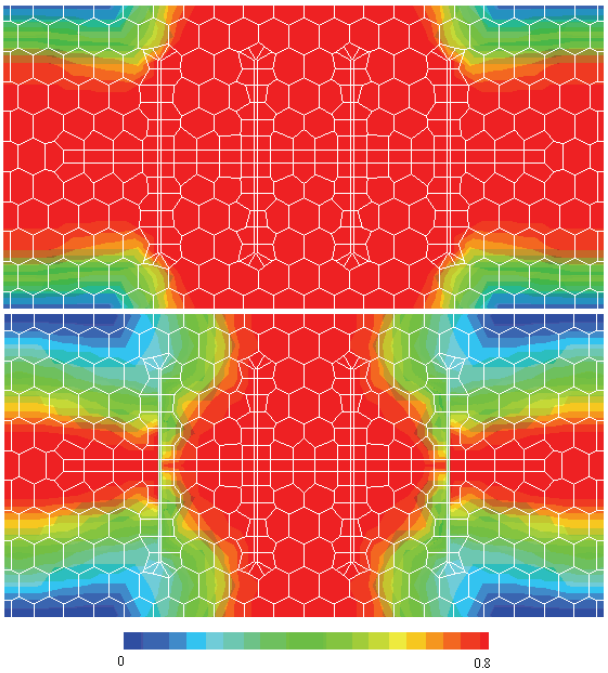

Figure 8: Oil saturation distribution for fractured horizontal well pattern (the angle between the fracture and the wellbore is 90°)

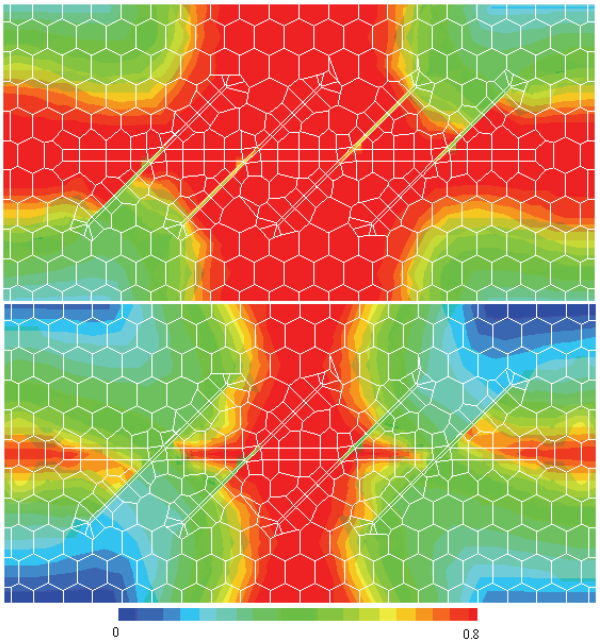

Figure 9: Oil saturation distribution for fractured horizontal well pattern (the angle between the fracture and the wellbore is 45°)

fractures encounter the water, the injected water was mainly produced from the outer fractures, which prove to be channels of low resistance, leading to the injected water advancing toward the inside fractures at reduced speed.

In Fig.9, all the four fractures are swept by injected water at the water-breakthrough time, the fracture edge closest to the injection well encounters water first, and then injected water advances toward the two middle factures. Meanwhile, there exists fluid flow in all directions for the PEBI grid, as it is a kind of locally orthogonal grid. Compared with the Cartesian grid, PEBI grid can simulate the fluid flow in a reservoir more accurately, by reducing the orientation effects. Due to the existence of the angle between the fracture and the wellbore, this region encounters water later. In addition, a residual oil region is easy to form between the injectors.

1. The effect of the half-length of fracture on production performance

   Assuming that there are four vertical fractures with a spacing of 150m, their influence on the cumulative oil production for different half-lengths of fracture is shown in Fig.10. In Fig.10, the cumulative oil production increases with the fracture length; the accretion magnitude however becomes smaller and smaller as the fracture half-length is bigger than 100m. Considering the cumulative oil production, the optimal half-length of a fracture ranges from 100m to 200m.

2. The effect of the number of fractures on production performance

   For a fractured horizontal well, the number of fractures is an important factor which affects the productivity. Assuming that the horizontal well length is 800m, and the fracture half-length is 150m, the relationship between the number of fractures and the cumulative oil production is shown in Fig.11. In Fig.11, for multiple fractures distributed along the horizontal wellbore, the cumulative oil production increases with the number of fractures. When the number of fractures exceeds 5 however, the enhancement of the production decreases due to the interference between the fractures. Therefore, more fractures do not necessarily mean a higher oil production, if the horizontal well length is fixed, and optimal fracture number is $3\sim5$.

3. The effect of the angle between the fracture and the wellbore on production performance

   The shape of a fracture is mainly determined by the geostatic pressure distribution. Actually, the wellbore of fractured horizontal well in the field is not horizontal, but just nearly horizontal due to the geological conditions and the employed drilling technology. Generally, the wellbore of fractured horizontal well cannot be guaranteed in the direction of maximum principal

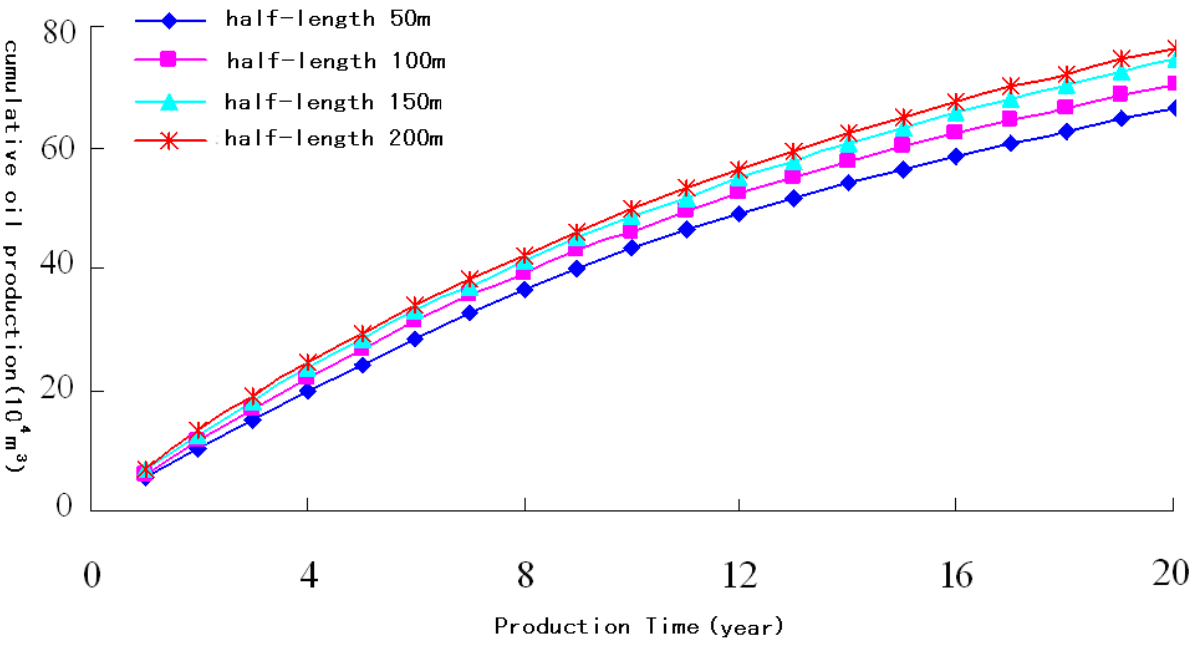

Figure 10: Cumulative oil production vs time for different fracture half-lengths

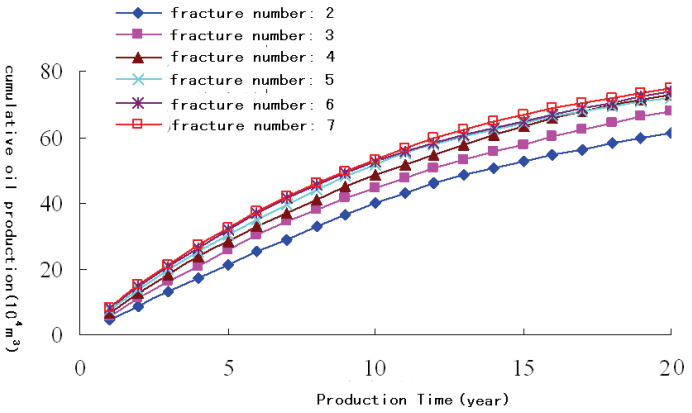

Figure 11: Cumulative oil production vs time for different fracture numbers

stress or minimum principal stress, causing an angle between the fracture and the wellbore during fracturing. To study the influence of angle between the fracture and the wellbore of fractured horizontal well on the production performance, we calculate the cumulative oil production under the conditions of 4 different fractures, with different angles, such as 30˚, 45˚, 60˚, 75˚ and 90˚, see Fig.12. In Fig.12, the cumulative oil production of a fractured horizontal well increases with the angle. As the angle increases, the perpendicular distance of fractures amplifies, which decreases the interference, that is, increases the effective drainage area of each well. Consequently, it is recommended to keep fracture direction perpendicular to the wellbore.

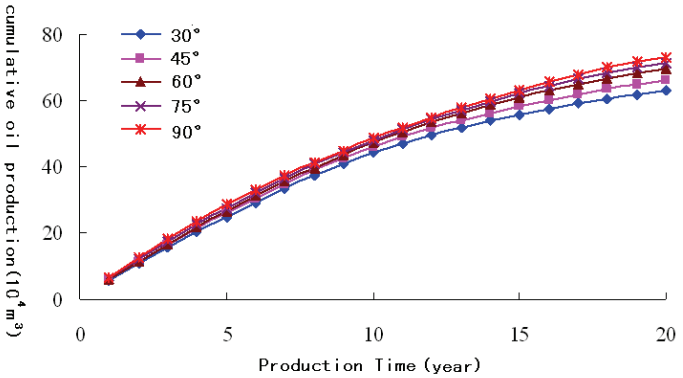

Figure 12: Cumulative oil production vs time for different angles

5 Conclusions

1. This paper proposed a technique for the generation of PEBI grid nodes, and a process for generating grid nodes at the junction of a fracture and the wellbore, or at the edge of a fracture for the fractured horizontal well. We have also constructed the PEBI grid nodes successfully based on the Delaunay triangulation. This method successfully solved the problems associated with the variation of the angle between the fracture and the wellbore, and the complicated fluid flow at the edges of fractures. The PEBI grid is more flexible as compared with the Cartesian grid, as it can distribute the grid nodes appropriately, based on the trajectory of horizontal well and the shapes of fractures, thus overcoming the flaws of the Cartesian grid in describing the shape of a fractured horizontal well.

2. This paper studied the production performance of a fractured horizontal well under a five-spot pattern condition, using the productivity prediction model based on the PEBI grid, and the calculations showed that: for a five-spot pattern, the fracture direction should be perpendicular to the horizontal well, since the fractured horizontal well is the production well, and the optimal fracture half-length is 100∼200m; the optimal number of fractures is 3∼5.

Acknowledgement: The author gratefully acknowledges the financial support of the national special project (Grant No: 2011ZX05009-005) and the Natural Science Foundation of China (NSFC, 51221003).

References

Chen, L.; Deng, M.R. (2011): Study on Algorithm of Statistics for Bolts Information of Steel Bridge and Iron Tower Based on Assembly Feature *AISS: Advances in Information Sciences & Service Sciences*, vol. 3, No. 10, pp.111.

Deng, H.; Bao, X.; Cheng, Z.X.; Wang, R.H. (2011): Numerical Well Testing Using Unstructured PEBI Grids *SPE 142258.*

Gonzalez K.; Bashbush J.L.; Rincon A. (2009): Simulation Study of Steamflooding With Horizontal Producers Using PEBI Grids. *SPE 121488*.

Heinemann ZE.; Brand C.W.; Chen, Y.M. (1991): Modeling Reservoir Geometry with Irregular Grids. *SPE 18412*.

Liu D.D.; Zhang J.; Liang J.Y. (2012): Research on the Dynamic Control of the Reservoir Limit Water Level Based on the Hydrological Information Automatic Telemeter-forecast System *AISS: Advances in Information Sciences & Service Sciences*, vol. 4, No. 13, pp.329336.

Melichar H.; Reingruber A.J.; Shotts DR.; Dobbs, W.C. (2003): Use of PEBI Grids for a Heavily Faulted Reservoir in the Gulf of Mexico. *SPE 84373*.

Palagi CL.; Ballin PR.; Aziz K (1993): The Modeling of Flow in Heterogeneous Reservoirs with Voronoi Grid. *SPE 25259*.

Patrick, W.P.; Ganzer, L.J. (2001): Reservoir Simulation Model for Fractured and Partially Fractured Reservoirs based on PEBI Grids *SPE 66384*.

Pedrosa J.; Oswaldo A.; Aziz K. (1986): Use of a hybrid grid in reservoir simulation. *SPE 13507*.

Verma S.; Aziz K. (1997): A Control Volume Scheme for Flexible Grids in Reservoir Simulation. *SPE 37999*.

Vestergaard H.; Olsen H.; Sikandar A.S.; Noman, R. (2008): The Application

of Unstructured-Gridding Techniques for Full-Field Simulation of a Giant Carbonate Reservoir Developed With Long Horizontal Wells. *SPE 120887*.